Jordan Journal of Dentistry,
DOI: https://doi.org/10.14525/JJD.96

Jordan Journal of Dentistry

https://jjd.just.edu.jo

Chronic Alcohol and Combination Antiretroviral Therapy Exacerbate Mandibular Bone Deterioration *via* Cytokine Dysregulation in Male Diabetic Sprague Dawley-Rats

Idemudia Eguavoen[1*], Ejikeme Felix Mbajiorgu[2], Robert Ndou[3]

1 Department of Anatomical Sciences, School of Biomedical Sciences, Faculty of Health Sciences, University of the Witwatersrand, Johannesburg, South Africa.
2 Department of Anatomical Sciences, School of Biomedical Sciences, Faculty of Health Sciences, University of the Witwatersrand, Johannesburg, South Africa.
3 Department of Human Anatomy and Histology, School of Medicine, Sefako Makgatho Health Sciences University, Pretoria, South Africa.

ARTICLE INFO

Article History:
Received: 18/8/2026
Accepted: 18/10/2026

Correspondence:
Idemudia Eguavoen, Department of Anatomical Sciences, School of Biomedical Sciences, Faculty of Health Sciences, University of the Witwatersrand, Johannesburg, South Africa.
dr_idemudia@yahoo.com
ejikeme.mbajiorgu@wits.ac.za

ABSTRACT

Objectives: Diabetes mellitus (DBT), chronic alcohol (ALC) consumption, and combination antiretroviral therapy (cART) can impair bone turnover, but their combined effects on mandibular bone cells and osteogenic cytokines remain unclear. This study evaluated these effects in male diabetic Sprague-Dawley rats.

Materials and Methods: Fifty-eight 10-week-old male rats were assigned to ten groups: control, ALC, DBT, cART, ALC+cART, DBT+ALC, DBT+cART, DBT+ALC+cART, gelatin (GEL), and buffered citrate (CB). ALC was administered as 10% v/v ethanol, and cART at 0.023 mg/kg daily for 12 weeks. Diabetes was induced with a 20% fructose diet and one Streptozotocin (STZ) injection (40 mg/kg), then confirmed by fasting blood glucose (>250 mg/dL) and serum insulin. We collected mandibles, fixed and decalcified them, and assessed them using haematoxylin and eosin (H&E) staining and immunohistochemistry for tartrate-resistant acid phosphatase, bone morphogenetic protein-3, and transforming growth factor-β1 (TRAP, BMP-3, and TGF-β1).

Results: ALC, cART, DBT, or their combinations increased bone marrow adiposity. BMP-3 inhibition reduced osteocyte numbers (TRAP-positive cells) without significantly changing TGF-β1 expression.

Conclusions: Diabetic conditions compounded by alcohol and cART exposure exacerbate bone deterioration through increased adipogenesis, reduced osteoblastogenesis, and enhanced osteolysis. These findings provide a biological basis for further investigating the oral effects of combined DBT, ALC, and cART on bone healing and implant osseointegration.

Keywords: Type-2 diabetes mellitus, Alcoholism, Combination antiretroviral therapy, Mandibular bone cells, Cytokines, Osteoblastogenesis, Osteolysis.

1. Introduction

Adipocytes, chondrocytes, and osteoblasts originate from a common progenitor, the bone marrow derived multipotent mesenchymal stem cells (MSCs). MSCs undergo lineage commitment and terminal differentiation into these mature cell types through tightly regulated intracellular signalling pathways (1,2). A delicate balance exists between adipogenesis and osteogenesis, where activation of one cell lineage often suppresses the other (2).

Multiple independent signalling pathways mediate this adipogenic-osteogenic differentiation of the

committed MSCs, including the transforming growth factor-β/bone morphogenetic protein (TGF-β/BMP) superfamily, Wingless and Int-1 (Wnt)/β-catenin, Hedgehog, Notch, and fibroblast growth factor (FGF) pathways, together with key transcription factors, such as peroxisome proliferator-activated receptor gamma (PPARγ), and runt-related transcription factor 2 (RUNX2) (1-3).

The Adipocytes (Ad) influence bone remodeling by the paracrine inhibitory effects of free fatty acids, adipokines, like resistin, leptin, adiponectin, and cytokines, such as tumor necrosis factor-alpha (TNF-α), interleukin-6 (IL-6), which influence the growth and function of MSC precursors as well as osteoblasts (Ob) and osteoclasts (Oc) (3). Adipogenesis impedes osteoblastogenesis, leading to increased bone marrow adipocytes (BMA), reduced levels of osteogenic cytokines, such as BMP-2 and insulin-like growth factor 1 (IGF-1), decreased bone formation, reduced trabecular bone mass, increased risk of osteoporosis, and increased bone fragility (1,2,4).

Diabetes mellitus (DBT), chronic alcohol (ALC) consumption, and combination antiretroviral therapy (cART) have been reported to promote the differentiation of bone marrow mesenchymal stem cells (BMMSCs) towards Ad instead of Ob (5-7). Individually, DBT, ALC, and cART have been shown to reduce bone turnover, reduce bone formation, and increase the risk of fracture (7-10).

TGF-β1 is one of the most abundant multi-functional osteogenic cytokines in the bone matrix (11,12), and it plays an important role in bone formation and remodeling by regulating the migration, proliferation, survival, and differentiation of osteoprogenitor cells, as well as the production and synthesis of extracellular matrix (ECM)(12).

TGF-β1 bone formation occurs through stimulating Ob proliferation by chemotactic attraction of Ob (13,14). It is an extracellular complex that is translocated into the intracellular domain to regulate bone cell differentiation (Ob and chondrocyte differentiation), to maintain bone homeostasis, and to maintain skeletal integrity after birth by pairing bone resorption and bone formation (12-14).

BMP-3 is a non-signalling molecule that competes via the TGFβ-Activin-like pathway, leading to the antagonism of pro-osteogenic BMP-2, 4, and 7-induced osteogenic cell commitment pathways. BMP-3 interacts with Wnt/β-catenin and TGF-β signalling; hence, it is a negative feedback regulator of bone formation (osteoblastogenesis), as it suppresses Ob maturation (15,16). Increased BMP-3 expression is associated with decreased bone mass, reduced trabecular volume, thinner cortical bone, and increased skeletal fragility; these features are commonly observed in type-2 diabetes mellitus (T2DM) (5-18).

Tartrate-resistant acid phosphatase (TRAP) is a reliable immunohistochemical (IHC) marker for osteocytes (Ocy) and their precursors involved in perilacunar remodeling and localized matrix demineralization (19). The presence of TRAP-positive Ocy is therefore indicative of active remodeling and bone homeostasis (19). During bone formation, proportions of Ob become embedded in the mineralized matrix and differentiate into Ocy (20). The Ocy are located in the lacunae or canaliculi near the site of mineralization at the periosteal surface. They form a dense, complex dendritic network that permits them to communicate with each other to exchange oxygen and nutrients, and also to communicate with other bone-forming cells or Ob by cytoplasmic processes in the lacuno-canaliculi network (LCN) (21,22). Embedded within an LCN, the Ocy serve as mechanosensors that regulate bone formation and resorption by coordinating Ob and osteoclasts (Oc) function (21,22). T2DM is known to disrupt this mechanosensing ability due to the impairment of the osteocytes' LCN signalling (20). T2DM disrupts LCN integrity and increases Ocy apoptosis, leading to reduced mechanosensing capability, impaired bone turnover, and increased fracture risk (20,23).

From dentistry perspective, impaired osteogenic activity and altered Oc function may adversely affect the ability of mandibular bone to respond to physiological and mechanical loading. This may be particularly relevant to alveolar bone, where continuous remodeling is required to maintain periodontal support and adapt to occlusal forces.

When diabetes coexists with harmful lifestyle behaviour, such as chronic ALC use or pharmacological challenges, such as cART, bone deterioration may be compounded. However, the synergistic effects of ALC and cART on adipogenesis, osteoblastogenesis, and osteolysis in the diabetic skeleton are yet to be understood.

This body of work aimed to evaluate whether ALC

intake with or without cART would adversely affect the number of Ad, Ocy, and the expression of TGF-β1 and BMP-3 in the mandibular bone of male diabetic Sprague-Dawley (SD) rats.

2. Materials and Methods

2.1 Chemicals and Reagents

Streptozotocin (STZ) (S0130) was purchased from Sigma-Aldrich Chemical Company (St. Louis, MO, USA), and Atripla, a fixed-dose combination antiretroviral drug, was purchased from Bristol–Myers Squibb and Gilead Sciences (Foster City, CA, USA). Serum analysis of insulin was conducted by enzyme-linked immunosorbent assay (ELISA) (Insulin ELISA kit; Rat INS E-EL-R3034, Elabscience® Houston, TX, USA).

2.2 Ethical Clearance

The protocol for this study was approved by the University of the Witwatersrand (Wits) Health Sciences Faculty's Higher Degree Committee. The Animal Research Ethics Committee (AREC), Wits University, approved this study (number: 2018/011/58/C) linked to the experimental site as Wits Research Animal Facility (WARF) in line with AREC guidelines.

2.3 Animal Housing

Eighty male SD rats (n=80), aged 10 weeks, were obtained from Charles River Laboratories (Wilmington, MA, USA) via the Central Animal Services (CAS), University of the Witwatersrand, Johannesburg, South Africa. Rats were housed individually in well-ventilated polycarbonate cages (430×220×200 mm) under specific pathogen-free conditions. Environmental parameters were maintained at a temperature of 21-23 °C with a 12-h light/12-h dark cycle and controlled relative humidity according to institutional animal facility standards. Standard rodent chow supplied by Labchef Nutrition Hub (Pty) Ltd (Stellenbosch, South Africa) and water were provided ad libitum. Rats were acclimatized for seven days prior to experimental dietary manipulation involving a 20% fructose diet. Cage bedding was changed three times weekly for non-diabetic rats and daily for diabetic rats to maintain hygiene and minimize infection risk.

2.4 Experimental Group Allocation and Treatment of Animals

Following acclimatization, rats were randomly allocated into ten experimental groups: untreated control, citrate buffer (CB), gelatine (GEL), ALC, DBT, cART, DBT+ALC, ALC+cART, DBT+cART, and DBT+ALC+cART (n=8 per group) (24). Group allocation was performed before intervention, and the individual rat served as the experimental unit. Final sample sizes ranged from n=6 to 8 per group due to mortality and exclusion based on diabetic status (Table 1). The sample size was considered sufficient to detect meaningful biological effects.

Table 1: Group allocation, sample size, and intervention

Group No	Experimental Group	Sample Size (n)	Intervention description
1.	Untreated Control	8	No intervention
2.	ALC	8	10% v/v ethanol in drinking water daily for 12 weeks
3.	DBT	7	Diabetes experimentally induced
4.	cART	8	Received cART
5.	DBT+ALC	6	Diabetes induction + alcohol administration
6.	ALC+cART	8	Alcohol administration + cART
7.	DBT+cART	7	Diabetes induction +cART
8.	DBT+ALC+cART	6	Diabetes induction+alcohol +cART

The CB group received 0.1 M CB. The solution consisted of 2.1 g citric acid ($C_6H_8O_7$) and 2.94g trisodium citrate dihydrate ($Na_3C_6H_5O_7 \cdot 2H_2O$) dissolved in 1 L of distilled water and adjusted to pH 4.5.

The cART was administered using ATRIPLA® (Bristol-Myers Squibb and Gilead Sciences, Foster City, CA, USA), a fixed-dose formulation containing emtricitabine (200 mg), tenofovir disoproxil fumarate (300 mg), and efavirenz (25). The administered dose was calculated as an extrapolated adult-equivalent dose of 0.023 mg/g body weight/day, adjusted according to individual animal body mass and delivered orally using medicated GEL cubes to ensure voluntary consumption (26). GEL cubes were freshly prepared using a

standardized formulation consisting of distilled water (5 mL), GEL powder (2 g), sugar (0.25 g), and beef-flavoured Bovril (0.1 g) to enhance palatability. The calculated cART dose was incorporated into the GEL mixture before solidification. Each animal received one GEL cube daily throughout the treatment period. Rats assigned to the GEL control group received identical GEL cubes prepared without antiretroviral (ARV) medication to control for vehicle exposure and handling effects.

2.5 Induction of Type-2 Diabetes Mellitus

T2DM was induced as previously reported by Owembabazi et al. (27) and Eguavoen et al. (28), followed by the modification of the procedure described by Wilson and Islam, 2012 (29). Animals received a 20% fructose-enriched diet prepared by mixing fructose (Nature's Choice™, Randvaal, South Africa) with standard chow and water to form pellets, which were dehydrated before feeding. This diet was administered for two weeks. Subsequently, animals received a single intraperitoneal (i.p.) injection of STZ (40 mg/kg body weight), freshly prepared in 0.05 M citrate buffer (pH 4.5). Seventy-two hours post-injection, fasting blood glucose (FBG) levels were measured. Rats with glucose levels ≥250 mg/dL were classified as diabetic. On confirmation of diabetes, rats were returned to a standard chow diet. Thus, to model T2DM, we used a 20% fructose diet in combination with a single i.p. dose of STZ (fructose-STZ) model to successfully reproduce the key pathophysiological features of T2DM.

FBG is measured biweekly after a 12-hour fast (20:00 am–08:00 pm). Hyperglycaemia was maintained throughout the 90-day study period.

Rats were weighed once a week and monitored daily for clinical signs of distress, illness, reduced mobility, or excessive weight loss.

2.6 Inclusion and Exclusion Criteria

All rats (n = 80) were normoglycaemic at baseline. Rats were excluded if they died, failed to develop diabetes, or did not maintain FBG>250 mg/dL during the 12-week study period.

Following exclusions, 58 rats distributed across eight experimental groups were included in the further analyses.

2.7 Termination Procedures and Bone Harvesting

At 24 weeks of age, rats were weighed and euthanized via i.p. administration of sodium pentobarbitone (250 mg/mL; Euthanyl™). Following confirmation of anaesthesia and loss of consciousness, approximately 4 mL of blood was collected via cardiac puncture. Blood samples were centrifuged at 3,000 rpm for 10 min, and the serum was separated, aliquoted into Eppendorf tubes, and stored at -80 °C until further analysis. Rats were subsequently perfused with 0.1 M phosphate-buffered saline (PBS; 0.9% NaCl) at a flow rate of 2 mL/min before mandible dissection and extraction.

2.8 Tissue Processing for Histological Staining

Bone samples were fixed in 10% neutral buffered formalin, decalcified in 20% (w/v) ethylenediaminetetraacetic acid (EDTA) (pH 7.4) for 10 days at 45°C, rinsed, and refixed before processing. Specimens were dehydrated and paraffin-embedded using an automated processor (Thermo Fisher Scientific Citadel 2000), oriented for anteroposterior sectioning, and cut at 5 µm using a rotary microtome (Leica Biosystems RM2125 RTS). Sections were stained with haematoxylin and eosin (H&E) for morphological assessment and Ad quantification, and subjected to immunohistochemical (IHC) analysis for TRAP, TGF-β1, and BMP-3.

Table 2. Primary and secondary antibodies used for immunohistochemistry

Antibody	Antibody type	Target	Dilutions	Incubation Conditions	Secondary Antibody	Code	Notes
TRAP	Primary	Osteocytes	1:100	Overnight at 4°C	Biotinylated Goat Anti-Rabbit IgG (H+L)	ab64256	Washed 3×5 min in PBS
BMP-3	Primary	ECM	1:400		Biotinylated Goat Anti-Rabbit IgG (H+L)	Overnight at 4 °C	Washed 3×5 min in PBS
TGF	Primary	ECM	1:75	Overnight at 4 °C	Biotinylated Goat Anti-Rabbit IgG (H+L)	ab64256	Washed 3×5 min in PBS

TRAP: tartrate-resistant acid phosphatase; BMP-3: bone morphogenetic protein-3; TGF: transforming growth factor; ECM: extracellular matrix.

2.9 Quantification of TRAP-positive Cells and Adipocytes in ROI (Region of Interest)

Photomicrographs were obtained using a light microscope (Carl Zeiss AG, Germany, Axioscope 2 Plus) equipped with an Axiocam HRC digital camera connected to a personal computer (Hewlett-Packard, South Africa). Images were captured from standardized regions of interest identified using H&E-stained sections to ensure consistent analysis. TRAP-positive Ocy (19,30) and Ad were identified according to established criteria in a previous study (31) and manually counted by the same investigator at different time points to confirm consistency and reproducibility.

2.10 TGF-β1 and BMP-3 Immunopositive Cells Intensity Grade Scoring Criteria

For each of these slides, representative high-power fields (HPFs) at magnification x 100 across the bone matrix region, avoiding poorly preserved or stained areas. For each HPF, estimation of the percentage of the immunopositive TGF-β1, and BMP-3 cells at each intensity category as: 0= no staining, 1= mild, 2=moderate stain, 3= intense in line with the method described by Price et al. (32). This scoring system utilizes the interaction of 3, 3′-diaminobenzidine (DAB) brown stain and haematoxylin (blue counterstain) to set thresholds of staining intensity between "0" (negative nuclei), "1+" (weakly positive nuclei), "2+" (moderately positive nuclei), and "3+ (strongly positive nuclei). The H-score calculations is based on the formula below where (P) represent percentage of cells (ranging from 0% to 100%), with P_0 being proportion of negative (0) cells (no stain); P_{1+} percentage of weakly stained cell nuclei; P_{2+} the percentage of 2+ cells, and P_{3+} the percentage of 3+ cells and summed as shown in the equation below:

H- Score equation= $(0 \times P_0) + (1 \times P_1) + (3 \times P_3)$.

2.11 Data Analysis

Data was managed using Microsoft Excel Office 365 (Microsoft Corporation) and analyzed using SPSS® version 28 (IBM Corp.). Normality was assessed using the Shapiro–Wilk test, which confirmed that the data was normally distributed. Accordingly, a one-way analysis of variance (ANOVA) followed by Fisher's least significant difference (LSD) post hoc test was used for multiple group comparisons. Ordinal immunopositivity intensity was semi-quantitatively scored as follows: no staining (0), mild (1), moderate (2), and intense (3). Statistical significance was set at $P < 0.05$.

3. Results

3.1 Fasting Blood Glucose

The FBG levels of the diabetic groups were significantly higher compared to the untreated, control, and non-diabetic groups ($p<0.05$) from the 2nd week to the 12th week. The highest FBG level was observed in the DBT+cART group, followed by the DBT, DBT+ALC, and the DBT+ALC+cART groups, respectively (Figure 1). FBG values exceeding 250 mg/dL were considered diabetic. The rats in both GEL and CB groups that had FBG and OGTT values <250mg/dL were considered non-diabetic and were subsequently excluded from the study (Figure 1).

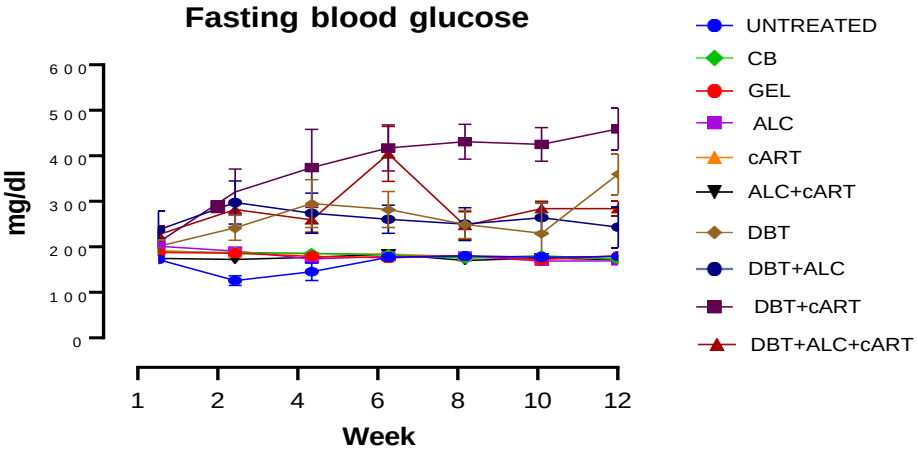


Figure 1: Fasting blood glucose level from 1 to 12 weeks

The FBG is significantly high in DBT, DBT+ALC, DBT+cART and DBT+ALC+cART against the untreated control and non-diabetic treated groups ($p<0.05$).

3.2 Serum Insulin Concentration Measurement

The Ins levels detected in the ALC+cART (1290pg/mL±146.6), ALC (1152pg/mL±150.3), and cART (1050pg/mL±18.83), were similar compared to the untreated control group (1251pg/mL±47.2) ($p=0.99$, $p=0.76$ and 0.08, respectively) (Fig. 2). On the contrary, DBT+cART (813.8pg/mL±92.2), DBT+ALC+cART (801.1pg/mL±85.59), DBT (771.2pg/mL±146.2) and the DBT+ALC (693pg/mL±52.87) groups had significantly lower Ins levels than the untreated control group ($p<0.001$ for all comparisons) (Figure 2). There was a reduction in Ins levels in diabetic rats, a feature that is a pancreatic beta cell failure symptom due to long-term hyperglycaemia.

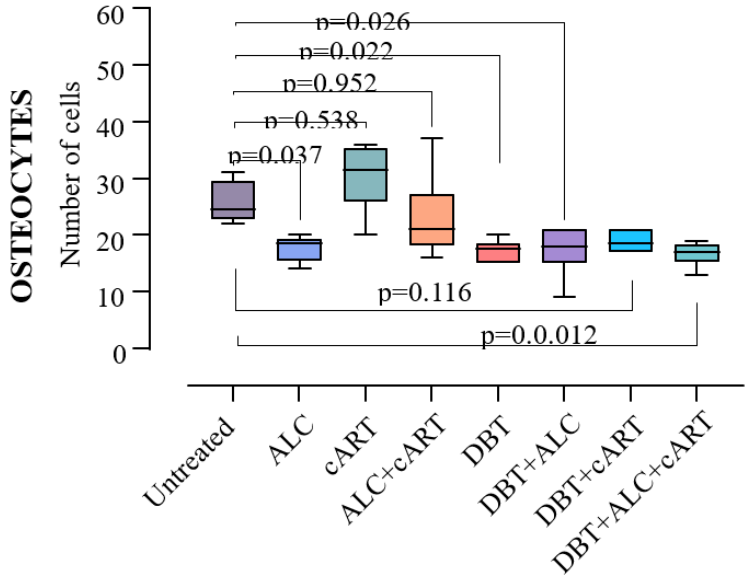


Figure 2: Serum insulin concentration at 12 weeks. Box-and-whisker plots of adipocyte quantity in various study groups. The line inside the box represents the mean, whereas the bottom and top lines of the box show the 25th and 75th percentiles, respectively. The whiskers below and above the box show the minimum and maximum values, respectively

A significant lower serum level was detected between the diabetic groups and the untreated control ($p<0.001$), while no significant difference in serum insulin level was detected between the non-diabetic group and the untreated control.

3.3 Mandibular Bone General Histological Appearance (Adipocyte Quantity)

The highest number of Ad was observed in the ALC+cART (38.33±4.80), cART (31.67±4.80), ALC (28.5±6.06), DBT+ALC (26.17±5.88), DBT (25.67±2.58), and DBT+cART (23.83±4.17). The DBT+ALC+cART (21.67±4.63) groups, which were significantly more than the untreated controls (11.67 ± 1.86) ($p<0.001$ for all the comparisons except $p=0.03$ for DBT+ALC+cART). The ALC group had similar values to the cART group ($p = 0.96$) (Figure 3). However, the ALC+cART group had significantly more Ad than the ALC group, but not the cART group ($p = 0.04$ and $p = 0.35$). The ALC+cART group also had significantly more Ad than the DBT, DBT+ALC, DBT+cART and DBT+ALC+cART ($P=0.002$, $P=0.004$, $P=0.001$ and $p<0.001$). The cART group showed more adipocytes only when compared to the DBT+ALC+cART ($p=0.03$) (Figure 3).

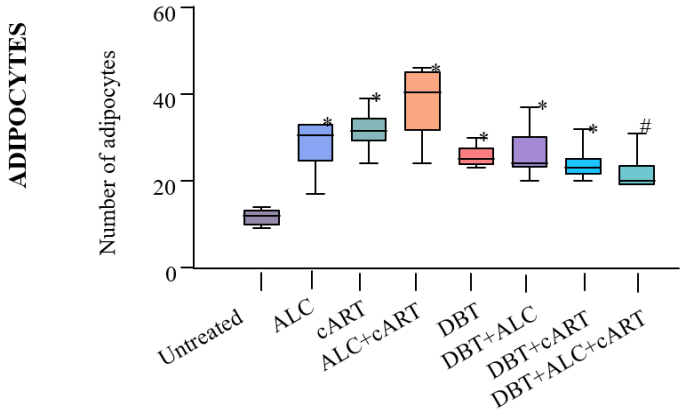


Figure 3: Number of adipocytes in the mandible**.** Box-and-whisker plots of adipocyte quantity in various study groups. The line inside the box represents the mean, whereas the bottom and top lines of the box show the 25th and 75th percentiles, respectively. The whiskers below and above the box show the minimum and maximum values, respectively.
***** p<0.001 vs untreated; # p=0.03 vs untreated.

ALC vs cART, ALC+cART, DBT+ALC, DBT+ALC+cART (p=0.96, p>0.04, p=0.10, p=0.32); cART vs ALC+cART, DBT+cART, DBT+ALC+cART (p=0.35, p=0.18, p=0.03, respectively); DBT vs ALC, cART, DBT+ALC, DBT+cART, DBT+ALC+cART (p<0.98, p=0.49, p>0.99, p=0.99 and p>0.99, respectively);DBT+ALC vs DBT+cART, DBT+ALC+cART (p=0.99, p>0.79, respectively).

3.4 Cells Expressing TRAP (Osteocyte Quantity)

The DBT+ALC+cART (16.67±2.07), DBT+ALC (17.33±4.45), DBT (18.17±2.64), and ALC (17.67±2.25) had the least number of TRAP immunopositive cells compared to the untreated controls (25.67±3.67) (p=0.01, p=0.03, p=0.022, p=0.04) (Figs. 4 and 5). These other groups: DBT+cART (18.83±1.84), ALC+cART (23.00±7.34), cART (30.33±6.02) groups were similar to the untreated group (p=0.114, p=0.95, p=0.54) (Figures 4 and 5).

The cART group had significantly more TRAP immunopositive cells than the ALC, DBT, DBT+ALC, and DBT+cART, DBT+ALC+cART groups (p<0.001) (Figures 4 and 5). There was no significant difference between the cART and the ALC+cART group (p=0.07). The DBT was similar to all other groups (Figures 4 and 5).

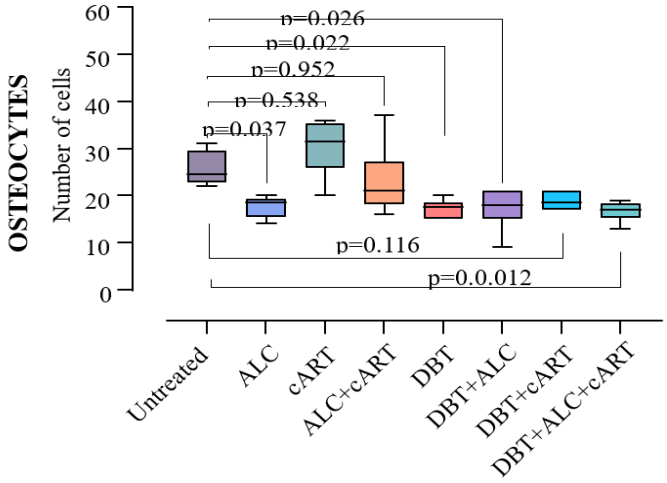


Figure 4: TRAP immunopositive cells quantity in the mandible**.** Box-and-whisker plots of TRAP mmunopositive cells in various study groups. The line inside the box represents the mean, whereas the bottom and top lines of the box show the 25th and 75th percentiles, respectively. The whiskers below and above the box show the minimum and maximum values, respectively

ALC vs cART, ALC+cART, DBT+ALC, DBT+ALC+cART ($p<0.001$, $p=0.37$, $p>0.99$, $p>0.99$); cART vs ALC+cART, DBT+cART, DBT+ALC+cART ($p=0.07$, $p<0.001$, $p<0.001$, respectively); DBT vs ALC, cART, DBT+ALC, DBT+cART, DBT+ALC+cART ($p>0.99$, $p<0.001$, $p>0.99$, $p>0.99$ and $p=0.98$, respectively); DBT+ALC vs DBT+cART, DBT+ALC+cART ($p=0.99$, for both comparisons)

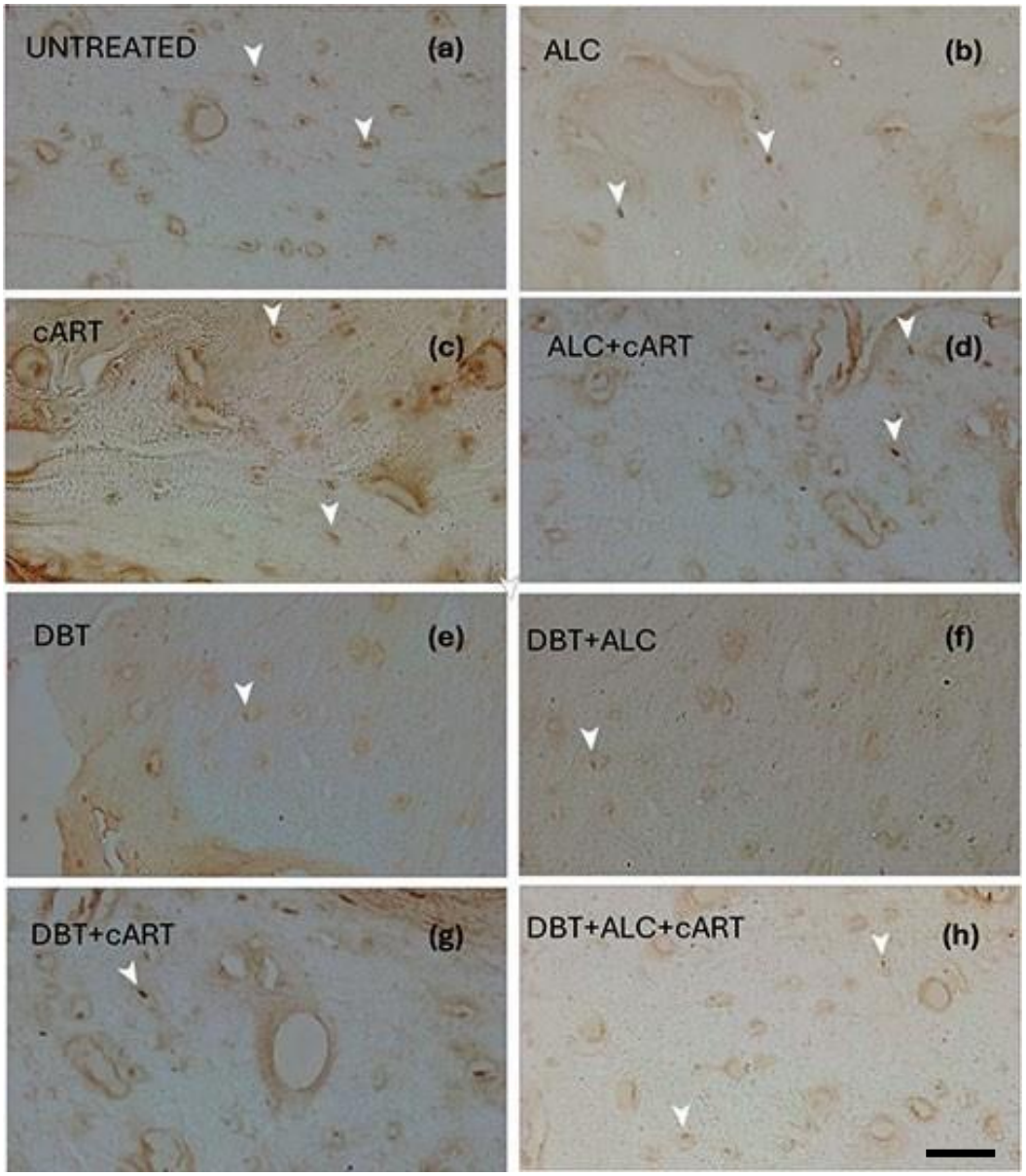


Figure 5: TRAP immunopositive osteocytes in the mandible. The Osteocytes are embedded in the bone matrix as depicted by the arrows and are found throughout a-h. Scale bar represents 40μm and applies to all micrographs

3.5 TGF-β1 Expression

None of the study groups exhibited an absence of TGF-β1 staining (Table 3 and Figure 6A). In the untreated control group, 50% of the samples showed mild staining, while the remaining 50% demonstrated moderate staining for TGF-β1. In the ALC group, 50% of the samples exhibited moderate staining and 16.7% showed intense staining; however, this was not significantly different from the untreated control group ($p = 0.05$).

In contrast, the cART group demonstrated a significant increase in TGF-β1 staining compared to the

untreated control group (p = 0.02), with 50% of the samples showing intense staining and 16.7% showing moderate staining. Although 66.7% of samples in the ALC+cART group exhibited moderate staining for TGF-β1, this was not significantly different from the untreated control group (p = 0.05).

The majority of samples in the DBT, DBT+ALC, DBT+cART, and DBT+ALC+cART groups demonstrated mild staining for TGF-β1, with no significant differences observed compared to the untreated control group (p= 0.62 for all groups except DBT+ALC+cART, where p = 0.32) (Table 3 and Figure 6A).

Table 3: TGF-β1 Immunopositivity

Groups	N	No stain		Mild		Moderate		Intense		P-value
		Count	%	Count	%	Count	%	Count	%	
Untreated	6	0	0	3	50.00	3	50.00	0	0	
ALC	6	0	0	1	16.70	3	50.00	2	33.30	0.05
cART	6	0	0	1	16.70	2	33.30	3	50.00	0.02
ALC+cART	6	0	0	0	0	4	66.70	2	33.30	0.05
DBT	6	0	0	4	66.70	2	33.30	0	0	0.62
DBT+ALC	6	0	0	4	66.70	2	33.30	0	0	0.62
DBT+cART	6	0	0	4	66.70	2	33.30	0	0	0.62
DBT+cART+ALC	6	0	0	5	83.30	1	16.70	0	0	0.32

ALC vs cART, ALC+cART, DBT+ALC, DBT+ALC+cART (p=0.620, p>0.99, p=0.02, p=0.01, respectively); cART vs ALC+cART, DBT+cART, DBT+ALC+cART (p=0.62, p=0.01, p=0.01, respectively); DBT vs ALC, cART, DBT+ALC, DBT+cART, DBT+ALC+cART (p<0.02, p=0.01, p>0.99, p>0.99 and p>0.99, respectively); DBT+ALC vs DBT+cART, DBT+ALC+cART (p=0.02, p>0.99, respectively).

3.6 BMP-3 Expressions

None of the study groups exhibited an absence of BMP-3 staining (Table 4 and Figure 6B). In the untreated control group, 50% of the samples demonstrated mild staining, while the remaining 50% showed moderate staining for BMP-3. In both the ALC and ALC+cART groups, 66.7% of the samples exhibited moderate staining. In contrast, only 16.7% of samples in the cART group demonstrated moderate staining, while the remaining samples showed mild staining. However, none of these groups (ALC, cART, and ALC+cART) differed significantly from the untreated control group (p = 0.66, p = 0.38, and p = 0.66, respectively) (Table 4).

In the DBT group, 66.7% of the samples exhibited intense BMP-3 immunostaining, which was significantly greater than that observed in the untreated control group (p = 0.01). Similarly, 50% of the samples in the DBT+ALC, DBT+cART, and DBT+ALC+cART groups demonstrated intense BMP3 immunostaining (Fig. 6B). Moderate staining was observed in 16.7% of samples in both the DBT+ALC and DBT+cART groups, while 50% of the DBT+ALC+cART samples exhibited moderate staining. These groups differed significantly from the untreated control group (p = 0.03, p = 0.03, and p = 0.01, respectively) (Table 4).

Furthermore, the ALC group differed significantly from both the DBT and DBT+ALC+cART groups, which exhibited a higher proportion of samples with intense BMP3 staining (p = 0.03 for both comparisons) (Table 4 and Figure 6B)

Table 4: BMP-3 Immunopositivity

Groups	N	No stain		Mild		Moderate		Intense		P value
		Count	%	Count	%	Count	%	Count	%	
Untreated	6	0	0	3	50.00	3	50.00	0	0	
ALC	6	0	0	2	33.30	4	66.70	0	0	0.66
cART	6	0	0	5	83.30	1	16.70	0	0	0.38
ALC+cART	6	0	0	2	33.30	4	66.70	0	0	0.66
DBT	6	0	0	1	16.70	1	16.70	4	66.70	0.01
DBT+ALC	6	0	0	1	16.70	2	33.30	3	50.00	0.03
DBT+cART	6	0	0	1	16.70	2	33.30	3	50.00	0.03
DBT+cART+ALC	6	0	0	0	0	3	50.00	3	50.00	0.01

ALC vs cART, ALC+cART, DBT+ALC, DBT+ALC+cART (p=0.19, p>0.99, p=0.08, p=0.003, respectively); cART vs ALC+cART, DBT+cART, DBT+ALC+cART (p=0.19, p=0.003, p=0.001, respectively); DBT vs ALC, cART, DBT+ALC, DBT+cART, DBT+ALC+cART (p<0.03, p=0.001, p=0.66, p=0.66 and p>0.99, respectively); DBT+ALC vs DBT+cART, DBT+ALC+cART (p=0.03, p=66, respectively).

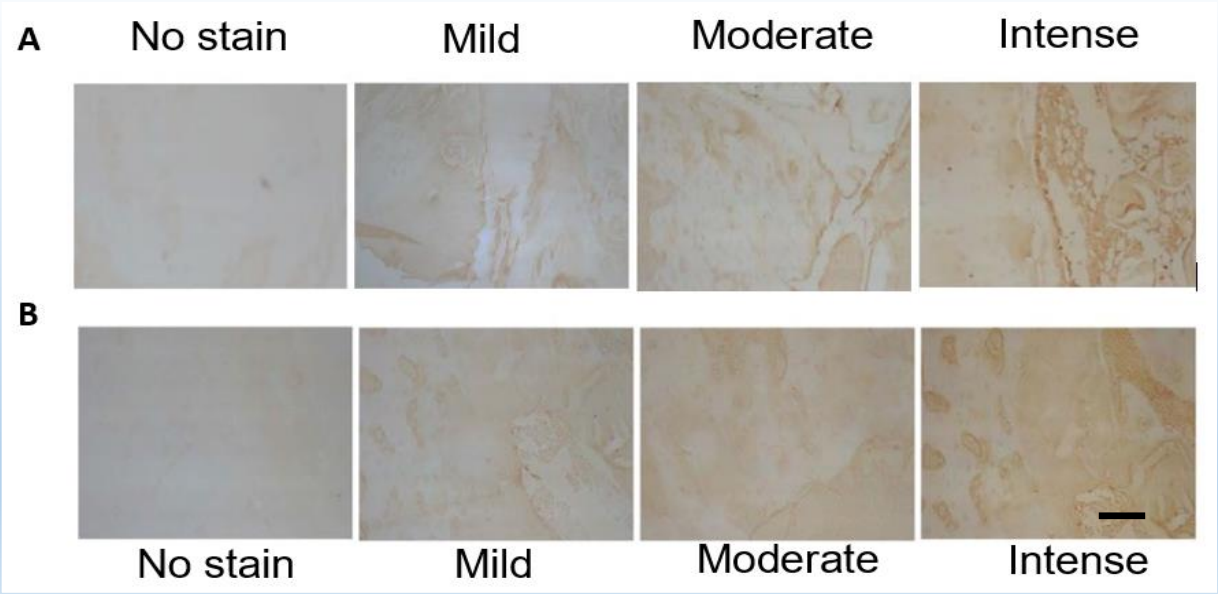


Figure 6: (A) Mandibular TGFβ1 immunopositivity graded, (B) Mandibular BMP-3 Immunopositivity graded. The grading was based on staining intensity. Scale bar represents 100μm and applies to all photomicrographs

4. Discussion

The results of this study showed that when diabetes was confounded by combination antiretroviral therapy and alcohol consumption (DBT+ALC+cART), pro-osteogenic cells (TRAP and TGF-β1) were negatively affected.

The BMA impairs skeletal integrity by favouring adipogenic lineage commitment at the expense of Ob differentiation (33,34). In this study, all experimental groups showed significantly elevated Ad accumulation compared to untreated controls. This result aligns with previous reports showing that alcohol use (5,34), diabetes (10,20,31,35), and antiretroviral therapy (ART) (36) reduce Ob activity and osteogenesis while promoting Ad formation. Expanded BMA encroach on available space for Ob precursors and secrete adipokines, such as adiponectin, which is anti-osteoblastic, pro-osteoclastic, and capable of inducing osteoblast apoptosis (11). Combined, these mechanisms reduce trabecular bone mass, impair bone formation, and increase fracture susceptibility. These effects are highly detrimental to the mandible, where structural

integrity is critical for oral function and implant stability. Moreover, Ad accumulation may diminish ART efficacy, as Ad can sequester ARV drugs, potentially worsening skeletal consequences in HIV-positive individuals receiving cART (36).

TRAP immunolabelling in bone can be used to assess ocy activity and the extent of perilacunar remodeling (19,21,30). The Ocy play an important role in coordinating the recruitment of Ocy and precursors and in initiating bone remodeling (36). TRAP-immunopositive cells contribute to the recruitment of Oc precursors to remodeling sites, thereby promoting bone matrix resorption and contributing to osteolysis (32,37). In the present study, the markedly reduced number of TRAP-positive Ocy observed in the DBT, DBT+ALC, and DBT+ALC+cART groups compared to the untreated controls suggests reduced Ocy density. This finding may indicate compromised LCN integrity and impaired mechanosensory function, both of which are essential for maintaining bone strength, adaptation to mechanical loading, and skeletal homeostasis (20,23).

Reduced osteogenic differentiation, together with impaired proliferation, differentiation, and survival of Ob, has previously been reported in DBT patients (38) and long-term ALC (39). Although a previous study reported increased TRAP-immunopositive cells in Zucker diabetic Sprague-Dawley (ZDSD) rats (35), these findings differ from those observed in the present study. The reason for this discrepancy remains unclear, but may be related to differences in rat species.

The reduced TRAP-positive cell counts observed in this study are likely associated with decreased Ocy numbers (40), possibly resulting from disrupted Ob maturation, a key determinant of Ocy formation. These findings further suggest impaired Ob lineage proliferation and differentiation in the diabetic treatment groups, leading to reduced Ocy density (19,23,30,37,40), decreased bone formation, enhanced osteolysis, and consequently increased bone fragility (1,20). Furthermore, the DBT+ALC+cART group exhibited the lowest number of TRAP-immunopositive Ocy, suggesting greater combined toxicity associated with DBT, ALC, and cART treatment. This observation supports the conclusion that combined exposure produced the most severe detrimental effects on bone quality and skeletal integrity.

In the present study, all diabetic groups (DBT, DBT+ALC, DBT+cART, and DBT+ALC+cART) exhibited intense BMP-3 staining compared to the untreated control and non-diabetic treated groups (ALC and cART). These findings corroborate previous reports of increased BMP-3 expression in ZDSD rats (35). Increased BMP-3 expression has been associated with diabetic bone pathology (17) and is known to impair Ob number and function, thereby increasing fracture risk (23).

BMP-3 has also been reported to be the most abundantly expressed BMP in demineralized bone, accounting for approximately 65% of total BMP content (16). BMP-3 functions as an anti-osteogenic cytokine that inhibits Ob differentiation through antagonism of pro-osteogenic BMP signalling pathways (12,16). The intense BMP-3 immunostaining observed in the present study is consistent with the reduced TRAP immunopositivity, as elevated BMP-3 expression is associated with impaired Ob differentiation and function. These anti-osteogenic effects contribute to reduced bone turnover, diminished bone mass, and increased bone fragility, which are characteristic features of diabetic skeletopathy (16-18).

The cART group was the only treatment group that demonstrated significantly greater TGF-β1 staining intensity compared to the untreated control group, whereas all other groups showed no significant differences. ALC consumption has previously been associated with elevated plasma TGF-β1 levels in alcoholic patients (39). In contrast, diabetes has been reported to suppress bone-derived TGF-β1 expression (7). A previous study using the ZDSD diabetic rat model similarly reported no significant differences in TGF-β1 expression (37). The findings of this study showed that ALC, DBT, and DBT+ALC did not significantly alter TGF-β1 expression.

The absence of significant changes in TGF-β1 expression should, however, be interpreted with caution. In the present study, extracellular TGF-β1 was assessed using IHC. This lack of change in TGF-β1 expression compared to the untreated controls may reflect the limitation of the method used to detect TGF-β1 expression rather than the true absence of altered signalling. This is a limitation for this study.

TGF-β signalling is initiated extracellularly, but requires intracellular Small Mothers Against Decapentaplegic (Smad) phosphorylation and subsequent nuclear translocation to regulate gene transcription and bone cell differentiation (15,16). Because IHC primarily

evaluates extracellular localization, it may not accurately reflect intracellular pathway activation. Consequently, unchanged extracellular TGF-β1 expression does not necessarily indicate preserved TGF-β signalling activity. Future studies evaluating intracellular active TGF-β1are necessary.

Taken together, the lack of significant changes in TGF-β1 expression, combined with elevated BMP-3 expression and reduced TRAP-positive Ocy, suggests an environment characterized by impaired Ob maturation, poor bone matrix remodeling, reduced bone turnover, diminished osteoblastogenesis, and increased osteolysis, particularly under conditions of combined DBT, ALC, and cART treatment.

These findings are invaluably significant in terms of dental and oral health. The mandible supports the teeth and provides the foundation for dental implants, making its bone quality and remodeling capacity important to oral health. Increased BMA, disruption of coordinated osteoblastogenesis, altered Ocy-associated remodelling, deposition of new bone, and increased BMP-3 immunoreactivity in the DBT groups, particularly the DBT+ALC+cART group, suggest changes in the mandibular bone microenvironment that could affect these functions. The findings support the potential value of integrating clinical assessment with appropriate dental radiographic imaging when planning dental implant placement, periodontal surgery, extraction, or other procedures involving alveolar and mandibular bone, especially when mandibular bone strength is required. As this study was conducted in an animal model, the findings cannot be directly extrapolated to clinical outcomes. However, they provide a biological basis for further investigating the oral effects of this co-existing factors.

5. Conclusions

DBT, ALC, and cART appeared to have combined detrimental effects on skeletal integrity. The DBT+ALC+cART group showed increased BMA, substantial Ocy loss, disruption of the LCN, and elevated BMP-3 expression. These findings suggest altered osteogenic signalling and compromised bone structure. Further studies should investigate how DBT, ALC, HIV, and cART interact with osteogenic cytokine signalling in the pathogenesis of bone disease.

Acknowledgements

The authors are grateful to the staff of the Central Animal Services, University of the Witwatersrand for animal husbandry including co-workers, Perry Vaughan and Jaclyn Asouzu Johnson.

Funding Information

The authors are grateful to the Faculty Research Committee Individual Research Grant for providing a Grant to partially support this work (grant no. 001.254.8421101 7th segment 5254).

Conflict of Interests

The authors declare no conflict of interests.

References

1. Akune T, Ohba S, Kamekura S, Yamaguchi M, Chung UI, et al. PPARγ insufficiency enhances osteogenesis through osteoblast formation from bone marrow progenitors. J Clin Invest. 2004;113:846-855.
2. Chen Q, Shou P, Zheng C, Jiang M, Cao G, et al. Fate decision of mesenchymal stem cells: Adipocytes or osteoblasts? Cell Death Differ. 2016;23:1128-1139.
3. Wu PH, Joseph G, Saeed I, Pirmoazen AM, Kenny K, et al. Bone marrow adiposity alterations in type-2 diabetes are sex-specific and associated with serum lipid levels. J Bone Miner Res. 2023;38:1877-1884.
4. Rharass T, Lucas S. Mechanisms in endocrinology: Bone marrow adiposity and bone, a bad romance? Eur J Endocrinol. 2018;179:R165-R182.
5. Wang Y, Li Y, Mao K, Li J, Cui Q, et al. Alcohol-induced adipogenesis in bone and marrow: A possible mechanism for osteonecrosis. Clin Orthop Relat Res. 2003; 410:213-224.
6. Kum JJY, Howlett CJ, Khan ZA. Dysregulated transforming growth factor-beta mediates early bone marrow dysfunction in diabetes. Commun Biol. 2022;5:1145.
7. Schinas G, Schinas I, Ntampanlis G, Polyzou E, Gogos C, et al. Bone disease in HIV: need for early diagnosis and prevention. Life (Basel). 2024;14:522.
8. Schousboe JT, Morin SN, Kline GA, Lix LM, Leslie WD. Differential risk of fracture attributable to type-2 diabetes mellitus according to skeletal site. Bone. 2022;154:116220.
9. Denys A, Norman A, Perrien DS, Suva LJ, Simon L, et

al. Impact of alcohol on bone health in people living with HIV: Integrating clinical data from serum bone markers with morphometric analysis in a non-human primate model. JBMR Plus. 2022;7:e10703.

10. Song F, Lee WD, Marmo T, Ji X, Song C, et al. Osteoblast-intrinsic defect in glucose metabolism impairs bone formation in type II diabetic male mice. Elife. 2023;12:e85714.
11. Chen J, Ning C, Mu J, Li D, Ma Y, et al. Role of Wnt signaling pathways in type-2 diabetes mellitus. Mol Cell Biochem. 2021;476:2219-2232.
12. Tang Y, Wu X, Lei W, Pang L, Wan C, et al. TGF-β1-induced migration of bone mesenchymal stem cell couples bone resorption with formation. Nat Med. 2009;15:757-765.
13. Ehnert S, Baur J, Schmitt A, Neumaier M, Lucke M, et al. TGF-β1 as possible link between loss of bone mineral density and chronic inflammation. PLoS One. 2010;5:e14073.
14. Yang Y, Zhang N, Lan F, Van Crombruggen K, Fang L, et al. Transforming growth factor-beta 1 pathways in inflammatory airway diseases. Allergy. 2014;69:699-707.
15. Daluiski A, Engstrand T, Bahamonde ME, Gamer LW, Agius E, et al. Bone morphogenetic protein-3 is a negative regulator of bone density. Nat Genet. 2001;27:84-88.
16. Kokabu S, Rosen V. BMP3 expression by osteoblast lineage cells is regulated by canonical Wnt signaling. FEBS Open Bio. 2018;8:168-176.
17. Gamer LW, Cox K, Carlo JM, Rosen V. Overexpression of BMP3 in the developing skeleton alters endochondral bone formation, resulting in spontaneous rib fractures. Dev Dyn. 2009;238:2374-2381.
18. Wang AN, Carlos J, Fraser GM, McGuire JJ. Zucker Diabetic-Sprague Dawley (ZDSD) rat: Type-2 diabetes translational research model. Exp Physiol. 2022;107:265-282.
19. Nakano Y, Toyosawa S, Takano Y. Eccentric localization of osteocytes expressing enzymatic activities, protein, and mRNA signals for type 5 tartrate-resistant acid phosphatase (TRAP). J Histochem Cytochem. 2004;52:1475-1482.
20. Picke AK, Campbell G, Napoli N, Hofbauer LC, Rauner M. Update on the impact of type-2 diabetes mellitus on bone metabolism and material properties. Endocr Connect. 2019;8:R55-R70.
21. Vashishth D, Verborgt O, Divine G, Schaffler MB, Fyhrie DP. Decline in osteocyte lacunar density in human cortical bone is associated with accumulation of microcracks with age. Bone. 2000;26:375-380.
22. Evans H, Andrews R, Abedi FA, Sprules A, Trend J, et al. Evidence for peri-lacunar remodeling and altered osteocyte lacuno-canalicular network in mouse models of myeloma-induced bone disease. JBMR Plus. 2024;8:ziae093.
23. Kaya S, Basta-Pljakic J, Seref-Ferlengez Z, Majeska RJ, Cardoso L, et al. Lactation-induced changes in the volume of osteocyte lacunar-canalicular space alter mechanical properties in cortical bone tissue. J Bone Miner Res. 2017;32:688-697. d
24. Anderson KD, Beckmann C, Heermant S, Ko FC, Dulion B, et al. Zucker diabetic-Sprague Dawley rats have impaired peri-implant bone formation, matrix composition, and implant fixation strength. JBMR Plus. 2023;7:e10819.
25. Julg B, Bogner JR. Atripla™-HIV therapy in one pill. Ther Clin Risk Manag. 2008;4:573-577.
26. Owembabazi E, Nkomozepi P, Calvey T, Mbajiorgu EF. Co-administration of alcohol and combination antiretroviral therapy (cART) in male Sprague Dawley rats: A study on testicular morphology, oxidative and cytokines perturbations. Anat Cell Biol. 2023;56:236-251.
27. Owembabazi E, Nkomozepi P, Mbajiorgu EF. Potential role of inducible nitric oxide synthase (iNOS) activity in testicular dysfunction following co-administration of alcohol and combination antiretroviral therapy (cART) in diabetic rats: an immunohistochemistry study. Toxicol Res. 2024;40:31-43.
28. Eguavoen I, Mbajiorgu EF, Perry V, Pillay D, Ndou R. Mandibular trabecular morphometry and tensile strength assessment in the diabetic Sprague Dawley rat consuming alcohol. Int J Morphol. 2024;42:1706-1712.
29. Wilson RD, Islam MS. Fructose-fed streptozotocin-injected rat: An alternative model for type-2 diabetes. Pharmacol Rep. 2012;64:129-139.
30. Dole NS, Mazur CM, Acevedo C, Lopez JP, Monteiro DA, et al. Osteocyte-intrinsic TGF-β signaling regulates bone quality through perilacunar/canalicular remodeling. Cell Rep. 2017;21:2585-2596.
31. Ferland-McCollough D, Maselli D, Spinetti G, Sambataro M, Sullivan N, et al. MCP-1 feedback loop between adipocytes and mesenchymal stromal cells causes fat accumulation and contributes to hematopoietic

stem cell rarefaction in the bone marrow of patients with diabetes. Diabetes. 2018;67:1380-1394.
32. Price P, Ganugapati U, Gatalica Z, Kakadekar A, Macpherson J, et al. Reinventing nuclear histo-score utilizing inherent morphologic cutoffs: Blue-brown color H-score (BBC-HS). Appl Immunohistochem Mol Morphol. 2023;31:500-506.
33. Gillet C, Dalla Valle A, Gaspard N, Spruyt D, Vertongen P, et al. Osteonecrosis of the femoral head: Lipotoxicity exacerbation in MSC and modifications of the bone marrow fluid. Endocrinology. 2017;158:490-502.
34. Johnson JT, Hussain MA, Cherian KE, Kapoor N, Paul TV. Chronic alcohol consumption and its impact on bone and metabolic health: A narrative review. Indian J Endocrinol Metab. 2022;26:206-212.
35. Dlamini GF, Ndou R. Osteoblastogenesis and osteolysis in the zucker diabetic Sprague Dawley rat humerus head. Anat Cell Biol. 2023;56:552-561.
36. Couturier J, Winchester LC, Suliburk JW, Wilkerson GK, Podany AT, et al. Adipocytes impair efficacy of antiretroviral therapy. Antiviral Res. 2018;154:140-148.
37. Bellido T. Osteocyte-driven bone remodeling. Calcif Tissue Int. 2014;94:25-34.
38. Phimphilai M, Pothacharoen P, Chattipakorn N, Kongtawelert P. The trajectory of osteoblast progenitor cells in patients with type-2 diabetes and the predictive model for their osteogenic differentiation ability. Sci Rep. 2023;13:2338.
39. Sampson HW. Alcohol's harmful effects on bone. Alcohol Health Res World. 1998;22:190-194.
40. Kim YK, Lee BC, Ham BJ, Yang BH, Roh S, et al. Increased transforming growth factor-beta1 in alcohol dependence. J Korean Med Sci. 2009;24:941-944.